NANO LETTERS

2004
Vol. 4, No. 6
1121−1125

Gold/Carbon Composite Tubes and Gold Nanowires by Impregnating Templates with Hydrogen Tetrachloroaurate/ Acetone Solutions

Petra Göring,[†] Eckhard Pippel,[†] Herbert Hofmeister,[†] Ralf B. Wehrspohn,[‡] Martin Steinhart,*[,†] and Ulrich Gösele[†]

Max Planck Institute of Microstructure Physics, Weinberg 2, D-06120 Halle, Germany, and Department of Physics, University of Paderborn,Warburger Strasse 100, D-33098 Paderborn, Germany

Received March 23, 2004

ABSTRACT

Carbon/gold composite nanotubes as well as gold nanorods were synthesized by the impregnation of porous alumina with diluted hydrogen tetrachloroaurate ($HAuCl_4$)/acetone solutions and subsequent thermolysis at moderate temperatures. Gold(III) is reduced, whereas carbon provided by the solvent acetone is oxidized. No oxygen and chlorine remain in the tube walls, which consist of gold nanocrystals supported by amorphous carbon. If the template pores have a diameter below a certain threshold value, which is of the order of 180 nm, single-crystalline gold nanowires are obtained. The methodology presented here may allow for synthesizing carbon tubes from ordinary acetone just by annealing.

Carbon nanotubes have extensively been studied since their discovery by Iijima.[1−5] Gold nanostructures have also attracted a great deal of interest because of the unique properties of this metal, for instance, its capability to form covalent bonds to thiol-functionalized organic compounds.[6] Gold nanoparticles[7−9] may be linked to DNA[10] and can be used as catalysts.[11,12] Several methods for the synthesis of gold nanowires and nanotubes containing gold, based on surfactant-directed growth of nanorods from spherical seeds,[13] and the exploitation of either sacrificial silver nanoobjects,[14,15] or porous materials[16−24] as templates, have been reported.

Recently, research efforts have been directed to the investigation of one-dimensional carbon/gold composites, because they may have specific electronic, photonic, and catalytic properties.[25,26] We report on a simple single-step approach for the synthesis of such materials that is neither costly nor time-consuming: impregnation of porous alumina with freshly prepared 1-wt % $HAuCl_4$/acetone solutions ($HAuCl_4 \cdot 3H_2O$, purchased from Merck). $HAuCl_4$ is a commonly used gold source and a strong oxidant. We dropped the solutions at ambient conditions on porous alumina. Note that the walls of such templates commonly consist of hydroxyl-terminated amorphous alumina.[27] It is well-known that $HAuCl_4$ is converted to gold at rather mild conditions, if it is in contact with a substrate having surface hydroxyl groups.[28,29] To accelerate the degradation of the gold precursor, the templates were annealed at 200 °C after the impregnation.

Figure 1a shows a scanning electron microscopy (SEM) image of impregnated self-ordered porous alumina[30−32] with a pore diameter of $D_p = 400$ nm and a pore depth of 100 μm, which was annealed at 200 °C for 1 h. The uppermost layer of the sample and the residual material on its surface were removed by sputtering with an argon plasma. The interior of the pores is still hollow, but some material is deposited on the pore walls. A treatment with aqueous KOH selectively etches alumina and releases nanotubes, which have an aspect ratio corresponding to that of the template pores even after annealing the impregnated templates for only five minutes (Figure 1b). Occasionally, the tubes were bent (Figure 1c), indicating that they have a ductile rather than a rigid and brittle nature. This may be the reason for the observation that their diameters seem to be larger than that of the template pores. They tubes are obviously flattened owing to their poor rigidity.

Figures 2a and b show bright-field transmission electron microscopy (TEM) images of a gold/carbon composite

* Corresponding author. E-mail: steinhart@mpi-halle.de.
[†] Max Planck Institute of Microstructure Physics.
[‡] University of Paderborn.

10.1021/nl049542v CCC: $27.50
Published on Web 05/08/2004

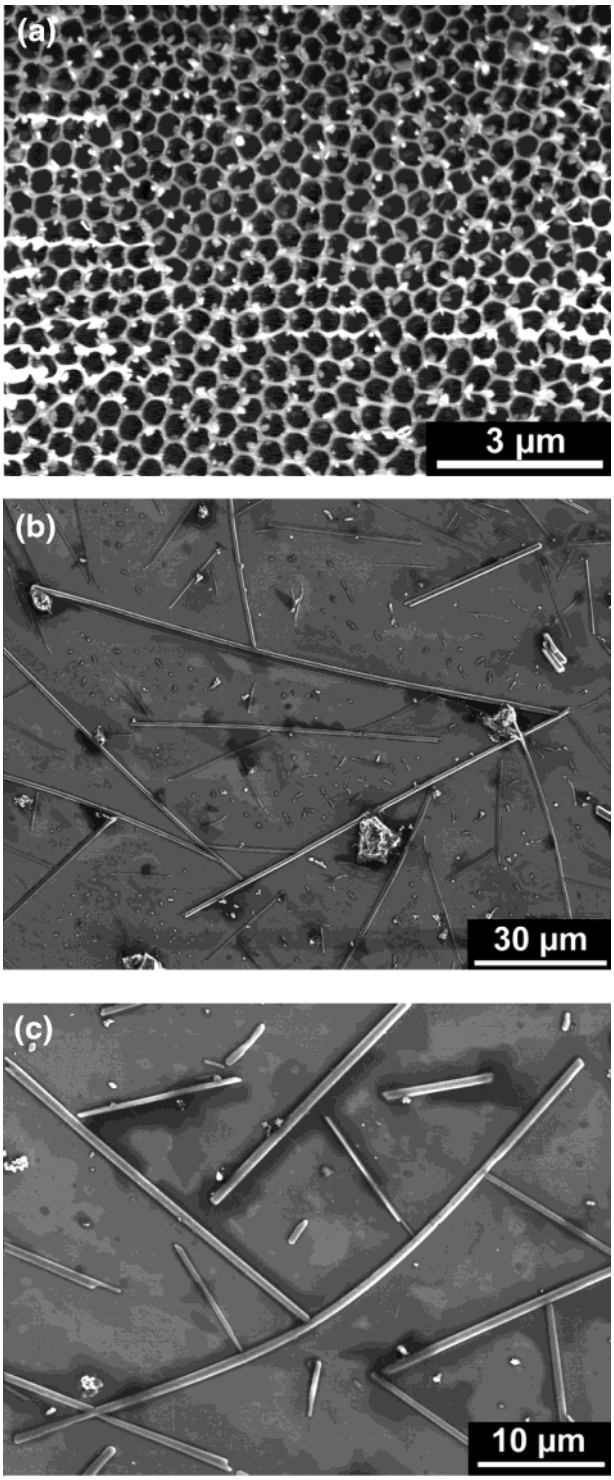

Figure 1. SEM micrographs of (a) porous alumina impregnated with a $HAuCl_4$/acetone solution, after annealing for 1 h at 200 °C and cleaning the surface by sputtering, and of (b), (c) released gold nanotubes prepared by annealing impregnated porous alumina (D_p = 400 nm, pore depth 100 microns) for five minutes at 200 °C.

nanotube prepared by annealing impregnated porous alumina ($D_p \approx 180$ nm) at 200 °C for 2 h and at 350 °C for 1 h at a lower and a higher magnification. The gold crystallites with a size of the order of 10 nm are discernible as bright spots in the corresponding dark-field image (Figure 2c). Again, the apparent diameter of the released tube is larger than that of the template pores, indicating that they are flattened. A high-resolution TEM image of individual gold nanoparticles within the wall of a gold/carbon composite tube, which was synthesized by annealing impregnated porous alumina (D_p = 400 nm) for 3 h at 200 °C, is pictured in Figure 2d. The matrix surrounding the gold particle does not show any lattice fringes and should thus be amorphous.

To probe the local chemical compostion of the tube walls, we recorded energy-dispersive X-ray (EDX) spectra on both a gold crystallite (Figure 3a) and the surrounding amorphous matrix (Figure 3b) of the tube shown in Figure 2d. The measurements unambiguously revealed the absence of oxygen, chlorine, and aluminum in the tube wall. Both spectra show copper peaks, which originate from the TEM grid on which the tube had been placed. They are more pronounced in the EDX spectrum of the gold nanocrystal, because the scattering of electrons causing the excitation of copper is higher for heavy metals. However, several peaks can be assigned to gold: M_α and M_β at 2.1 keV, L_α at 9.7 keV and L_b at 11.4 keV. The carbon peak obviously originates from the opposite side of the tube wall, or the surroundings. The spectrum recorded on the amorphous area (Figure 3b) only exhibits a strong carbon peak (K_α and K_β at 0.3 keV). Electron energy loss spectroscopy (EELS) (Figure 3c) confirmed the exclusive presence of carbon in the amorphous areas. The energy loss near edge structure (ELNES) of the carbon K-edge recorded on a tube prepared like those depicted in figures 1b and c exhibits the characteristic features of amorphous carbon: a peak at 283 eV that can be assigned to sp^2 hybridized carbon atoms, and a stronger, rather broad peak at 295 eV that corresponds to sp^3 hybridized carbon. Analyzing the corresponding low loss spectrum revealed that the thickness of the tube walls is of the order of 30 nm. Note that both the EELS and EDX spectra, which were performed with a Philips CM20FEG transmission electron microscope operating at an accelerating voltage of 200 kV, were taken on tube segments having no supporting carbon film of the TEM grid underneath.

From these findings it can be concluded that the tubes consist of discrete Au crystallites supported by an amorphous carbon matrix. The pore walls of the template may act as a catalyst during their formation, but do not degrade even though $HAuCl_4$ is a rather aggressive oxidant. Otherwise, the tube walls should contain considerable amounts of aluminum and oxygen. The most plausible explanation for the absence of chlorine and oxygen is the formation of thermodynamically stable, volatile species such as HCl or carbon oxides. The only source providing carbon for the tube walls to come into question is acetone. Indeed, only discrete gold nanocrystals, but no tubular structures, were obtained when aqueous solutions containing $HAuCl_4$ were used for impregnating the templates. Therefore, the carbon of the methyl groups of acetone was oxidized by replacing C−H bonds by C−C bonds in the course of the nanotube formation.

We have varied D_p systematically from 900 to 55 nm. Tubes were exclusively obtained for pore diameters of 900 and 400 nm, respectively. Figure 4a shows, for instance, a

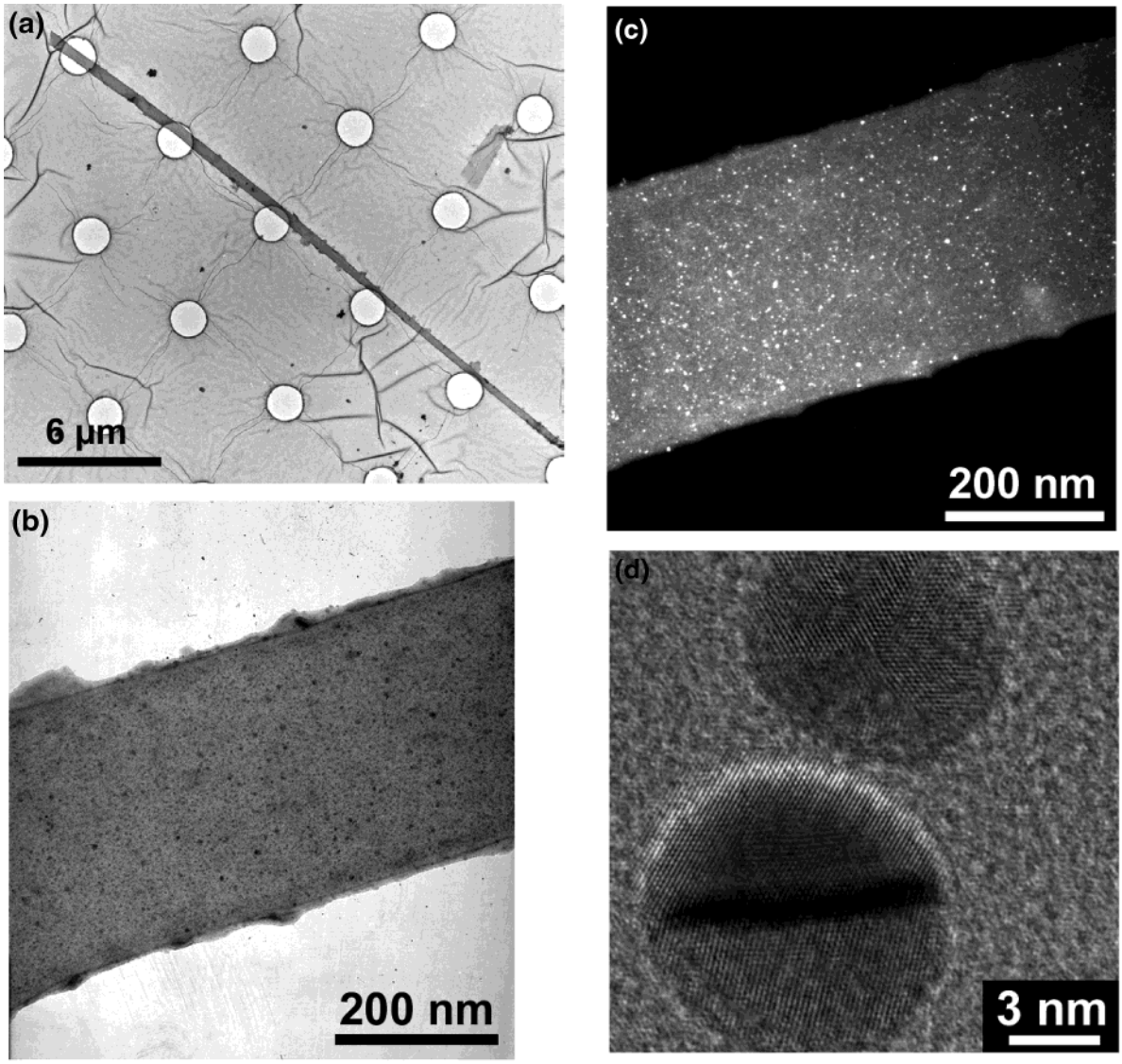

Figure 2. TEM micrographs of a released gold/carbon composite nanotube prepared by impregnating porous alumina ($D_p \approx 180$ nm) with a $HAuCl_4$/acetone solution and annealing at 200 °C for 2 h and at 350 °C for 1 h: (a) overview, (b) bright-field, and (c) dark-field image of a wall detail. (d) High-resolution TEM image of individual gold nanoparticles within the wall of a gold/carbon composite tube, synthesized by annealing impregnated porous alumina with $D_p = 400$ nm for 3 h at 200 °C.

segment of a tube obtained by annealing impregnated macroporous silicon[33] ($D_p = 900$ nm, the maximum pore diameter currently attainable for ordered porous alumina is 400 nm) for 3 h at 200 °C. Despite the relatively large diameter, tubular structures were conserved even after the removal of the template. However, since deposition of $HAuCl_4$ into mesoporous hosts commonly yields Au nanorods,[34,35] it is expected that a crossover from tubes to rods occurs if D_p is reduced below a certain threshold value. The applied annealing protocol may also play a role, since the mobility of gold clusters and their tendency to coalesce strongly depend on the temperature. The sample prepared by annealing impregnated porous alumina ($D_p = 180$ nm) at 200 °C for 2 h and at 350 °C for 1 h contained a considerable amount of solid gold rods. The TEM micrograph (Figure 4b) shows a nanotube (on the top) and a solid gold nanorod (at the bottom). The selected area electron diffraction (SAED) pattern of a segment of the nanorod (Figure 4c) can be ascribed to a face-centered cubic gold single-crystal viewed along the ⟨111⟩ direction. Besides the regular diffraction spots of the {220} and {422} type, the SAED pattern exhibits fractional 1/3{422} spots being kinematically "forbidden", but expected to appear in thin films, nanoparticles and nanowires.[36,37] Further reducing the diameter of the template pores to 55 nm resulted in the exclusive formation of solid gold nanorods. A typical example for this is displayed in Figure 4d. No nanoobjects consisting of or containing carbon could be found in this case, although this sample was, apart from the pore diameter of the template, prepared in the same manner as that shown in Figure 4b.

The underlying chemical and physical processes that guide the formation of the obtained one-dimensional gold/carbon and gold nanoobjects are far from being understood. It is, however, an intriguing perspective to exploit these phenomena for the synthesis of customized nanostructures. This is

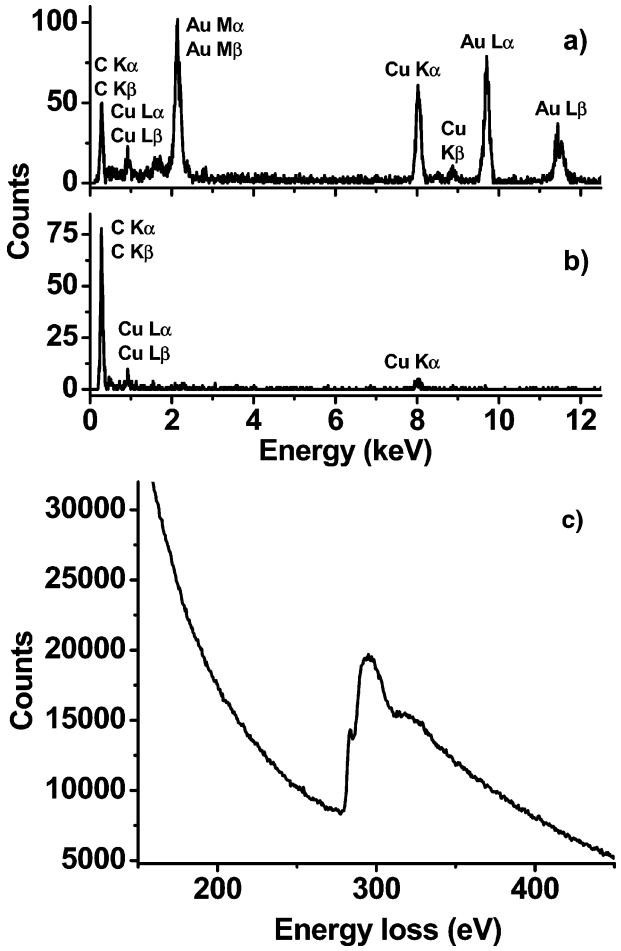

Figure 3. Energy-dispersive X-ray (EDX) spectra on (a) a gold crystallite in the wall of the tube shown in Figure 2d and (b) on the amorphous matrix. The copper peaks originate from the TEM grid on which the tube had been placed. (c) ELNES of the carbon K-edge recorded on an amorphous area of a gold/carbon tube prepared like that shown in figures 1b and c. The peak at 283 eV can be assigned to sp^2 hybridized and that at 295 eV to sp^3 hybridized carbon. All the measurements were performed with a Philips CM20FEG transmission electron microscope operating at an accelerating voltage of 200 kV on tube segments having no supporting carbon film of the TEM grid underneath.

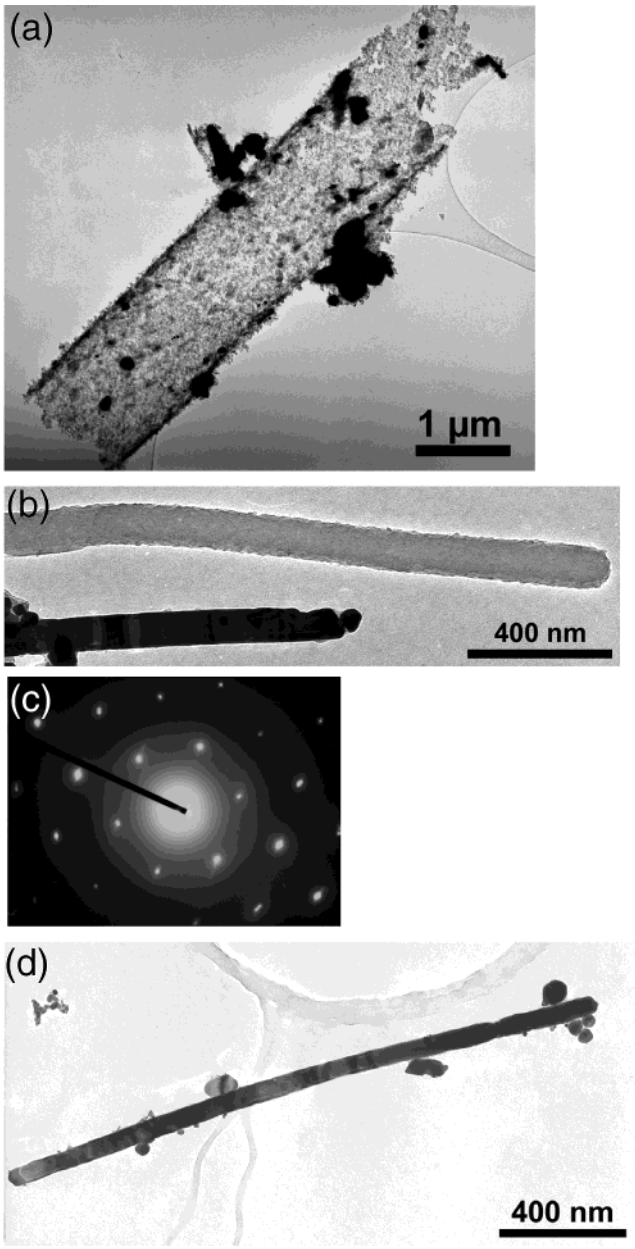

Figure 4. TEM micrographs of released gold/carbon nanotubes and wires synthesized by impregnating templates with different pore diameters with a $HAuCl_4$/acetone solution. (a) Tube prepared by annealing impregnated macroporous silicon (D_p = 900 nm, pore depth 100 microns) for 3 h at 200 °C. (b) Sample prepared by annealing impregnated alumina (D_p = 180 nm) at 200 °C for 2 h and at 350 °C for 1 h. A nanotube can be seen on top and a solid nanorod at the bottom. (c) SAED pattern of a segment of the nanorod shown in Figure 2b. (d) Nanorod prepared by annealing impregnated alumina (D_p = 55 nm) at 200 °C for 2 h and at 350 °C for 1 h.

all the more the case since the methodology presented here provides an inexpensive and, regarding its preparative complexity, rather simple access to gold nanowires and gold/carbon composite tubes. If we consider, for instance, hexagonal porous alumina with a lattice constant of 500 nm and a pore diameter of 400 nm, there are 460,000,000 pores per square centimeter with an overall pore volume of approximately 6 μL. Taking into account the density of acetone, which is 0.8 kg/L and a concentration of $HAuCl_4$ of 1 wt %, we need 0.05 μg $HAuCl_4$ to obtain 460,000,000 carbon tubes decorated with gold nanoparticles. Their further functionalization, for example, by converting the amorphous carbon into graphite, is under investigation. In the end, it may be possible to synthesize carbon tubes from ordinary acetone just by annealing.

Acknowledgment. Support from the German Ministry of Education and Science (Nanobiotechnologie FKZ 031 200 2A) is gratefully acknowledged. We thank S. Hopfe for sputtering some samples.

References

(1) Iijima, S. *Nature* **1991**, *354*, 56.
(2) Ebbesen, T. W.; Ajayan, P. M. *Nature* **1992**, *358*, 220.
(3) Amelinckx, S.; Zhang, X. B.; Bernaerts, D.; Zhang, X. F.; Ivanov, V.; Nagy, J. B. *Science* **1994**, *265*, 635.

(4) Terrones, M.; Grobert, N.; Olivares, J.; Zhang, J. P.; Terrones, H.; Kordatos, K.; Hsu, H. K.; Hare, J. P.; Townsend, P. D.; Prassides, K.; Cheetham, A. K.; Kroto, H. W.; Walton, D. R. M. *Nature* **1997**, *388*, 52.
(5) Ren, Z. F.; Huang, Z. P.; Xu, J. W.; Wang, J. H.; Bush, P.; Siegal, M. P.; Provencio, P. N. *Science* **1998**, *282*, 1105.
(6) Bain, C. D.; Troughton, E. B.; Tao, Y.-T.; Evall, J.; Whitesides, G. M.; Nuzzo, R. G. *J. Am. Chem. Soc.* **1989**, *111*, 321.
(7) Brust, M.; Walker, M.; Bethell, D.; Schiffrin, D. J.; Whyman, R. *J. Chem. Soc., Chem. Commun.* **1994**, *801*.
(8) El-Sayed, M. A. *Acc. Chem. Res.* **2001**, *34*, 257.
(9) Schmid, G.; Corain, B. *Eur. J. Inorg. Chem.* **2003**, 3081.
(10) Mirkin, C. A.; Letsinger, R. L.; Mucic, R. C.; Storhoff, J. J. *Nature* **1996**, *382*, 607.
(11) Mohr, C.; Hofmeister, H.; Claus, P. *J. Catal.* **2003**, *213*, 86.
(12) Mohr, C.; Hofmeister, H.; Radnik, J.; Claus, P. *J. Am. Chem. Soc.* **2003**, *125*, 1905.
(13) Busbee, B. D.; Obare, S. O.; Murphy, C. J. *Adv. Mater.* **2003**, *15*, 414.
(14) Sun, Y.; Xia, Y. *Science* **2002**, *298*, 2176.
(15) Sun, Y.; Mayers, B. T.; Xia, Y. *Nano Lett.* **2002**, *2*, 481.
(16) Brumlik, C. J.; Martin, C. R. *J. Am. Chem. Soc.* **1991**, *113*, 3174.
(17) Martin, C. R. *Adv. Mater.* **1991**, *3*, 457.
(18) Martin, C. R. *Science* **1994**, *266*, 1961.
(19) Menon, V. P.; Martin, C. R. *Anal. Chem.* **1995**, *67*, 1920.
(20) Martin, B. R.; Dermody, D. J.; Reiss, B. D.; Fang, M.; Lyon, L. A.; Natan, M. J.; Mallouk, T. E. *Adv. Mater.* **1999**, *11*, 1021.
(21) Matthias, S.; Schilling, J.; Nielsch, K.; Müller, F.; Wehrspohn, R. B.; Gösele, U. *Adv. Mater.* **2002**, *14*, 1618.
(22) Wirtz, M.; Martin, C. R. *Adv. Mater.* **2003**, *15*, 455.
(23) Tian, M.; Wang, J.; Kurtz, J.; Mallouk, T. E.; Chan, M. H. W. *Nano Lett.* **2003**, *3*, 919.
(24) Lahav, M.; Sehayek, T.; Vaskevich, A.; Rubinstein, I. *Angew. Chem., Int. Ed.* **2003**, *42*, 5576.
(25) Kim, K.; Lee, S. H.; Yi, W.; Kim, J.; Choi, J. W.; Park, Y.; Jin, J.-I. *Adv. Mater.* **2003**, *15*, 1618.
(26) Carrillo, A.; Swartz, J. A.; Gamba, J. M.; Kane, R. S.; Chakrapani, N.; Wei, B.; Ajayan, P. M. *Nano Lett.* **2003**, *3*, 1437.
(27) Braunstein, P.; Kormann, H. P.; Meyer-Zaika, W.; Pugin, R.; Schmid, G. *Chem. Eur. J.* **2000**, *6*, 4646.
(28) Hofmeister, H.; Miclea, P.-T.; Mörke, W. *Part. Part. Syst. Charact.* **2002**, *19*, 359.
(29) Kan, C.; Cai, W.; Li, Z.; Fu, G.; Zhang, L. *Chem. Phys. Lett.* **2003**, *382*, 318.
(30) Masuda, H.; Fukuda, K. *Science* **1995**, *268*, 1466.
(31) Masuda, H.; Yada, K.; Osaka, A. *Jpn. J. Appl. Phys., Part 2* **1998**, *37*, L1340.
(32) Jessensky, O.; Müller, F.; Gösele, U. *Appl. Phys. Lett.* **1998**, *72*, 1173.
(33) Lehmann, V. *J. Electrochem. Soc.* **1993**, *140*, 2836.
(34) Li, Z. S.; Kan, C. X.; Cai, W. P. *Appl. Phys. Lett.* **2003**, *82*, 1392.
(35) Araki, H.; Fukuoka, A.; Sakamoto, Y.; Inagaki, S.; Sugimoto, N.; Fukushima, Y.; Ichikawa, M. *J. Mol. Catal. A: Chem.* **2003**, *199*, 95.
(36) Nihoul, G.; Abdelmoula, K.; Metois, J. J. *Ultramicroscopy* **1984**, *12*, 353.
(37) Golan, Y.; Margulis, L.; Hodes, G.; Rubinstein, I.; Hutchison, J. L. *Surf. Sci.* **1994**, *311*, L633.

NL049542V